Self-Assembled Growth of $PbTiO_3$ Nanoparticles into Microspheres and Bur-like Structures

Guozhong Wang,[†] Ragnhild Sæterli,[‡] Per Martin Rørvik,[†] Antonius T. J. van Helvoort,[‡] Randi Holmestad,[‡] Tor Grande,[†] and Mari-Ann Einarsrud*[,†]

Department of Materials Science and Engineering and Department of Physics, Norwegian University of Science and Technology (NTNU), 7491 Trondheim, Norway

Received December 21, 2006. Revised Manuscript Received February 20, 2007

Novel bur-like hierarchical nanostructures of $PbTiO_3$ were prepared by hydrothermal synthesis. Surfactants containing phenyl-sulfonic groups resulted in self-assembly of nanocrystals. In absence of the surfactant, monodisperse $PbTiO_3$ microspheres were formed. The microspheres were 1−5 μm in diameter, and consisted of ∼20 nm tetragonal $PbTiO_3$ crystals. The microspheres were formed by primary nucleation of $PbTiO_3$ nanocrystals followed by aggregation into microspheres. The hierarchical bur-like nanostructures exhibit a unique geometry consisting of a microsphere core with an outer shell of nanorods. The nanorods, which grow along the [001] direction, were ∼50−100 nm in diameter and from several hundreds of nanometers up to 2 μm in length. A mechanism for the growth of the bur-like nanostructures was proposed. First, agglomeration of $PbTiO_3$ nanocrystals into microspheres occurs. $PbTiO_3$ mesocrystals are formed at the surface of the microspheres by self-assembly of cube-shaped or facetted $PbTiO_3$ nanocrystals, and the mesocrystals ripen and grow further into nanorods.

1. Introduction

Among functional ternary oxide materials, lead titanate ($PbTiO_3$) is an important ferroelectric material with a Curie temperature, T_c, of 490 °C. $PbTiO_3$-based materials are widely applied in electronics as multilayer capacitors, nonvolatile memories, resonators, and ultrasonic transducers, as a result of a large pyroelectric coefficient and a relatively low permittivity.[1] $PbTiO_3$ particles have successfully been synthesized using a variety of methods, such as sol−gel process,[2] hydrothermal method,[3] and solid-state mixing method.[4] These particles are mostly nonspherical, such as tabular, plate, and cube shaped. Recently, $PbTiO_3$ microspheres have been prepared by a two step process where TiO_2 microspheres formed in a first step were converted to $PbTiO_3$ by a hydrothermal reaction in a lead acetate solution.[5] In contrast to the multistep approaches, one-step strategies that combine synthesis with in situ assembly are highly desired for simplicity and for the robust structures that often are formed.[6]

The production of one-dimensional (1D) $PbTiO_3$ nanomaterials has lingered far behind the preparation of particles and thin films, and to date only a limited number of papers have been published on 1D nanomaterials, such as nanofibers, nanotubes,[7] and nanowires.[8] The assembly of 1D nanomaterials into three-dimensional (3D) hierarchical nanostructures has only been achieved in a recent communication from the present group.[9] Because the ferroelectric properties of $PbTiO_3$ depend on size and shape of the materials,[10] controlling the particle size, monodispersity, microstructure, and morphology are important concerns in developing techniques for synthesizing $PbTiO_3$. Although there are several well-established methods available for preparation of nanoparticles and 1D nanomaterials assembly, such as DNA and biological template,[11] polymer-controlled reaction,[6,12]\ chemical vapor deposition,[13] and reverse micro-

* To whom correspondence should be addressed. E-mail: mari-ann.einarsrud@material.ntnu.no.
[†] Department of Materials Science and Engineering.
[‡] Department of Physics.

(1) (a) Jaffe, W.; Cook, R., Jr.; Jaffe, H. *Piezoelectric Ceramics*; Academic Press: New York, 1971. (b) Dawber, M.; Rabe, K. M.; Scott, J. F. *Rev. Mod. Phys.* **2005**, *77*, 1083−1130.
(2) (a) Paris, E. C.; Leite, E. R.; Longo, E.; Varela, J. A. *Mater. Lett.* **1998**, *37*, 1−5. (b) Kim, S.; Jun, M. C.; Hwang, S. C. *J. Am. Ceram. Soc.* **1999**, *82*, 289−296.
(3) (a) Moon, J.; Carasso, M. L.; Krarup, H. G.; Kerchner, J. A.; Adair, J. H. *J. Mater. Res.* **1999**, *14*, 866−875. (b) Cho, S. B.; Noh, J. S.; Lencka, M. M.; Riman, R. E. *J. Eur. Ceram. Soc.* **2003**, *23*, 2323−2335. (c) Gersten, B.; Lencka, M.; Riman, R. *Chem. Mater.* **2002**, *14*, 1950−1960.
(4) (a) Udomporn, A.; Ananta, S. *Mater. Lett.* **2004**, *58*, 1154−1159. (b) Mandal, T. K.; Gopalakrishnan, J. *J. Mater. Chem.* **2004**, *14*, 1273−1280. (c) Idrissi, H.; Aboujalil, A.; Deloume, J. P.; Fantozzi, G.; Durand, B. *J. Eur. Ceram. Soc.* **1999**, *19*, 1997−2004.
(5) Choi, J. Y.; Kim, C. H.; Kim, D. K. *J. Am. Ceram. Soc.* **1998**, *81*, 1353−1356.
(6) Calderone, V. R.; Testino, A.; Buscaglia, M. T.; Bassoli, M.; Bottino, C.; Viviani, M.; Buscaglia, V.; Nanni, P. *Chem. Mater.* **2006**, *18*, 1627−1633.
(7) Hernandez-Sanchez, B. A.; Chang, K. S.; Scancella, M. T.; Burris, J. L.; Kohli, S.; Fisher, E. R.; Dorhout, P. K. *Chem. Mater.* **2005**, *17*, 5909−5919.
(8) (a) Lu, X.; Zhang, D.; Zhao, Q.; Wang, C.; Zhang, W.; Wei, Y. *Macromol. Rapid Commun.* **2006**, *27*, 76−80. (b) Hu, Y. M.; Gu, H. S.; Sun, X. C.; You, J. *Appl. Phys. Lett.* **2006**, *88*, 193120-1−193120-3.
(9) Wang, G. Z.; Sæterli, R.; Rørvik, P. M.; Helvoort, A. T. J.; Holmestad, R.; Grande, T.; Einarsrud, M. A. *J. Nanosci. Nanotechnol.* **2007**, in press.
(10) (a) Jiang, B.; Peng, J. L.; Bursill, L. A.; Zhong, W. L. *J. Appl. Phys.* **2000**, *87*, 3462−3467. (b) Streiffer, S. K.; Eastman, J. A.; Fong, D. D.; Thompson, C.; Munkholm, A.; Ramana Murty, M. V.; Auciello, O.; Bai, G. R.; Stephenson, G. B. *Phys. Rev. Lett.* **2002**, *89*, 067601-1−067601-4. (c) Chattopadhyay, S.; Ayyub, P.; Palkar, V. R.; Multani, M. *Phys. Rev. B* **1995**, *52*, 13177−13183.

10.1021/cm063047d CCC: $37.00
Published on Web 03/31/2007

emulsions,[14] use of nanoparticle-based transformations as routes to the formation of high-order $PbTiO_3$ architectures from aqueous solution are rare. Here we report a simple synthesis approach to build new complex $PbTiO_3$ structures: bur-like 3D hierarchical nanostructures and microspheres, obtained by in situ self-assembly of $PbTiO_3$ nanoparticles under hydrothermal conditions using sodium dodecylbenzene sulfonate (SDBS) or poly(sodium 4-styrenesulfonate) (PSS) surfactant. We show how the sol−gel approach combined with hydrothermal treatment can be applied to grow complex nanostructures. Complex multimetal oxide nanostructures prepared by this mechanism have the potential as components for functional nanostructures and are also potentially interesting for electronic studies and applications.

2. Experimental Section

2.1. Synthesis. *2.1.1. Precursor Synthesis.* Titanium citrate solution was formed by dissolution of titanium(IV) isopropoxide (8.6 mL, 98%, Acros Organic, U.S.A.) in a 5.26 M aqueous solution of citric acid (CA; BDH Laboratory supplies, U.K.) at 60 °C and pH ≈ 5 (CA to metal molar ratio equal to 3). Stoichiometric amounts of lead acetate (10.70 g, 99%, Research Chemical, Ltd., U.S.A.) dissolved in 45 mL of CO_2-free deionized water was then added to the Ti−citrate solution. Ethylene glycol (EG; CA to EG molar ratio equal to 0.44) was added as polymerization agent, and then the mixture was kept under slow stirring until a clear Pb−Ti−citrate sol was obtained. Upon continued heating at ∼90 °C to remove the water, the Pb−Ti−citrate sol became more viscous, without any visible phase separation. After about 6 h, a polymeric dried gel was obtained.

2.1.2. Hydrothermal Synthesis Using Pb−Ti−Citrate Sol as Precursor. The Pb−Ti−citrate sol was used as the precursor for further hydrothermal synthesis. The mineralization reagent potassium hydroxide was added to adjust the pH from 9 to above 14. Concentrations of 0.1, 0.2, or 0.3 M of one of the following surfactants was used: SDBS, cetyltrimethyl ammonium bromide (CTAB), PSS, naphthyl phosphate potassium (NPP), cysteamine *s*-phosphate sodium (CSS; all Merck Schuchardt OHG, Germany), or sodium dodecyl sulfate (SDS; Sigma-Aldrich, Inc., U.S.A.). After stirring for 30 min, the reaction mixture (about 30 mL) was sealed in a Teflon lined stainless steel autoclave (4748 Large Capacity Autoclave, 125 mL, Parr Instrument Company, IL) and heated to a temperature in the range 90−200 °C under the auto-generated pressure for 4−48 h. After cooling to room temperature, the products were washed several times with distilled water and ethanol, and the product was dried at 80 °C for 12 h.

2.1.3. Hydrothermal Synthesis Using Dried Gel as Precursor. The dried gel obtained from the Pb−Ti−citrate sol was also used as a precursor for hydrothermal synthesis. The dried gel precursor (0.01 mol) was added to 5 M KOH (20 mL) aqueous solution containing 0.2 M of the surfactant SDBS or CTAB. After stirring for 30 min, the reaction mixture (about 30 mL) was sealed in a Teflon lined stainless steel autoclave and heated to a temperature in the range 100−150 °C under the auto-generated pressure for 24 h. After cooling to room temperature, the product was washed several times with distilled water and ethanol and dried at 80 °C for 12 h.

2.2. Characterization. The products were analyzed by X-ray diffraction (XRD), in a 2θ range from 20° to 80°, using Cu Kα radiation (Philips PW 1730/10). The surface area of the samples was determined by nitrogen adsorption (Micrometrics ASAP 2000) using the five-point BET isotherm. The morphology of the prepared $PbTiO_3$ was studied by scanning electron microscopy (SEM, Hitachi S-3500N), field emission scanning electron microscopy (FESEM, Hitachi S-4300SE), and field emission transmission electron microscopy (TEM, JEOL-2010F, 200 kV) with an energy-dispersive X-ray spectrometer (EDS, OXFORD, Link ISIS) and an electron energy loss spectrometer (EELS, Gatan Imaging Filter). The powders were dispersed in ethanol using ultrasonic vibration. The samples for microscopy studies were prepared by deposition of dispersions of the powder in ethanol directly on the SEM stubs or holey carbon for TEM examination. The cross-section TEM samples were made by embedding the particles in epoxy resin and thereafter sliced by a microtome to a thickness of about 50 nm. The thin slices were put on a TEM copper grid.

3. Results

3.1. Synthesis and Assembly of Spherical Aggregates of $PbTiO_3$ Nanoparticles. XRD patterns of the products synthesized by hydrothermal treatment of the Pb−Ti−citrate sol without surfactant for 24 h at different reaction temperatures are shown in Figure 1a. At 90 °C, an amorphous product was formed, while above 100 °C the product became crystalline $PbTiO_3$ consistent with literature (JCPDS No. 06-0452). Significant peak broadening was observed for the materials prepared at lower temperatures. From the Scherrer equation, the crystallite size at 100, 110, 130, 150, and 180 °C was calculated to be 15, 16, 18, 19, and 20 nm, respectively.

SEM images of the products obtained after 24 h at various reaction temperatures are shown in Figure 2. The product transformed from individual particles to microspheres with increasing reaction temperature. The products obtained at 90 °C and 100 °C (Figure 2a,b) were almost only nanoparticles, but a few microspheres were also present. TEM examination of the products at 100 °C (inset of Figure 2b) showed the primary particle size of ∼5 nm. The reaction product at 110 °C (Figure 2c) consisted of microspheres (diameter from 1 μm to 4.5 μm) and a limited number of nanoparticles. At 130 °C, the product was only microspheres (Figure 2d), and the size became more uniform (∼ 1.5 μm) with increasing reaction temperature to 150 °C (Figure 2e). The microspheres consisted of aggregated nanoparticles; see inset in Figure 2e. The $PbTiO_3$ nanoparticles constituting the microspheres were ∼22 nm in diameter calculated from

(11) (a) Iwaura, R.; Minamikawa, H.; Shimizu, T. *J. Colloid Interface Sci.* **2004**, *277*, 299−303. (b) Manzanera, M.; Frankel, D. J.; Li, H.; Zhou, D.; Bruckbauer, A.; Kreutzmann, P.; Blackburn, J. M.; Abell, C.; Rayment, T.; Klenerman, D.; Barker, P. D. *Nano Lett.* **2006**, *6*, 365−370. (c) Nuraje, N.; Su, K.; Haboosheh, A.; Samson, J.; Manning, E. P.; Yang, N. L. *Adv. Mater.* **2006**, *18*, 807−811.

(12) (a) Yu, S. H.; Antonietti, M.; Cölfen, H.; Hartmann, J. *Nano Lett.* **2003**, *3*, 379−382. (b) Wohlrab, S.; Pinna, N.; Antonietti, M.; Cölfen, H. *Chem.—Eur. J.* **2005**, *11*, 2903−2913.

(13) (a) Gao. P.; Wang, Z. L. *J. Phys. Chem. B* **2002**, *106*, 12653−12658. (b) Lao, J. Y.; Wen, J. G.; Ren, Z. F. *Nano Lett.* **2002**, *2*, 1287−1291. (c) Yan, H.; He, R.; Johnson, J.; Law, M.; Saykally, R. J.; Yang, P. *J. Am. Chem. Soc.* **2003**, *125*, 4728−4729. (d) Wang, D.; Qian, F.; Yang, C.; Zhong, Z.; Lieber, C. M. *Nano Lett.* **2004**, *4*, 871−874. (e) Dick, K. A.; Deppert, K.; Larsson, M. W.; Martensson, T.; Seifert, W.; Wallenberg, L. R.; Samuelson, L. *Nat. Mater.* **2004**, *3*, 380−384.

(14) (a) Li, M.; Schnablegger, H.; Mann, S. *Nature* **1999**, *402*, 393−395. (b) Shi, H.; Qi, L.; Ma, J.; Cheng, H.; Zhu, B. *Adv. Mater.* **2003**, *15*, 1647−1651. (c) Thachepan, S.; Li, M.; Davis, S. A.; Mann, S. *Chem. Mater.* **2006**, *18*, 3557−3561.

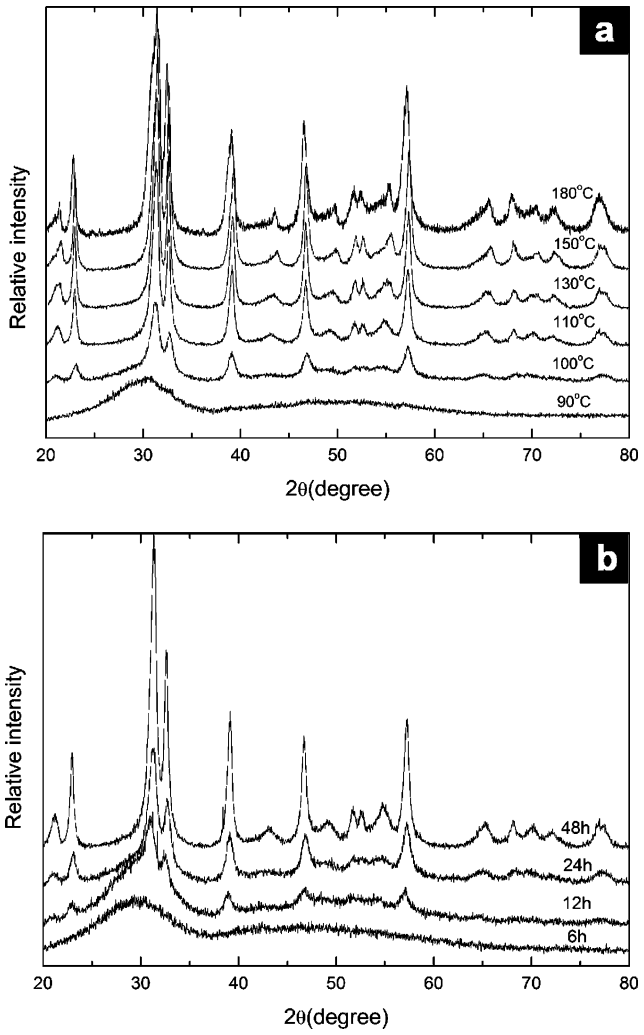

Figure 1. XRD patterns of the products prepared by the hydrothermal method from Pb−Ti−citrate sol without surfactant: (a) at different reaction temperatures for 24 h and (b) at 100 °C for different reaction times.

surface area (S_{BET} = 35 m^2/g) assuming spherical particles. The diameter of the microspheres increased to ∼4 μm at 180 °C as shown in Figure 2f.

To further study the kinetics of the microsphere formation, experiments were performed at 100 °C for different reaction times. XRD results evidenced that the degree of crystallinity of the reaction product is increasing with increasing reaction time (6, 12, 24, and 48 h) at 100 °C (Figure 1b). The amorphous material prepared after 6 h exhibited a fine particulate structure. The crystalline nanoparticles formed after more than 12 h were increasingly assembled into microspheres with diameter from 1.5 μm to 2 μm (increasing with reaction time). After 48 h at 100 °C there were still a large number of individual nanoparticles present (Figure 3). The evolution of the morphology and crystallinity of the products formed as a function of reaction time is similar to the evolution of products obtained using different reaction temperatures. By increasing the reaction temperature to 150 °C, only microspheres similar to the ones shown in Figure 2e were achieved even with only 4 h of reaction time.

Addition of EG at pH ≥ 14 was necessary for the formation of tetragonal perovskite $PbTiO_3$. Otherwise, cubic $Pb_2Ti_2O_6$ and $PbCO_3$ were formed. Apparently, EG is important for assembling the nanoparticles into spherical aggregates. By using the $PbTiO_3$ dried gel instead of the sol as precursor, only tetragonal perovskite nanoparticles without microspheres were formed and no aggregation into microspheres occurred.

3.2. Bur-like $PbTiO_3$ Structures. XRD revealed that crystalline tetragonal $PbTiO_3$ was obtained during hydrothermal synthesis for 48 h at 180 °C with addition of the surfactant SDBS (concentration of 0.1, 0.2, and 0.3 M) to the Pb−Ti−citrate sol. The corresponding morphology of the products is shown in Figure 4a−d, where enlarged parts of the nanostructures are provided as insets. Using 0.1 M SDBS, nanoparticles, microspheres, and bur-like nanostructures were observed. The microspheres consisted of nanoparticles (Figure 4a) and the bur-like nanostructures (Figure 4b) showed clearly a core−shell structure. The core consisted of a microsphere of nanoparticles while the shell consisted of nanorods growing from the core in the radial direction as shown in the inset of Figure 4b. Perfect bur-like nanostructures with diameters from 2.5 μm to 5 μm were formed by increasing the SDBS concentration to 0.2 M. A single bur-like nanostructure, as shown in Figure 4c, is composed of uniform prismatic nanorods with diameter of ∼100 nm and length up to 1 μm as shown in the inset in Figure 4c. Increasing the SDBS concentration to 0.3 M, bur-like $PbTiO_3$ nanostructures (Figure 4d) were formed with nanorods (diameters ∼ 70 nm, length ∼ 2 μm, inset in Figure 4d) having a prismatic tetragonal shape and a well-faceted tip. Without the addition of surfactant, only microspheres with a diameter ∼ 4.5 μm were formed after 48 h at 180 °C as shown in Figure 4e. The presence of SDBS is therefore a prerequisite for the growth of nanorods.

Experiments with 0.2 M SDBS for 48 h at 150 °C and 200 °C were carried out to investigate the effect of reaction temperature. At 150 °C, the products had a bur-like nanostructure where short nanorods were adhered to the surface of a microsphere as shown in Figure 4f. However, increasing the temperature to 200 °C lead to the formation of bur-like nanostructures composed of needle-like $PbTiO_3$ nanorods as shown in Figure 4g. These nanorods with sharp ends (inset in Figure 4g) had diameters of ∼80 nm and length of ∼1.5 μm. All nanorods taper from the bottom to the tip.

We also studied the effect on morphology by varying the reaction time, type of surfactant, and precursor. Experiments were performed at 180 °C with 0.2 M SDBS for 6, 12, and 24 h. XRD revealed that the degree of crystallinity of the reaction product was increasing with increasing reaction time. The amorphous material prepared after 6 h exhibited a fine particulate structure. Increasing the reaction time to 12 h, both crystalline nanoparticles and some microspheres were formed. A further extension of the reaction time to 24 h resulted in the appearance of bur-like nanostructures. The evolution of the morphology of the products formed as a function of reaction time is similar to the evolution of products obtained with different SDBS concentrations. When the surfactant SDBS was replaced by SDS, PSS, NPP, or CSS, only the products using the surfactant PSS consisted of the bur-like nanostructures (Figure 4h), while the products using the other surfactants were nanoparticles or microspheres. The cationic surfactant CTAB (0.2 M) resulted in

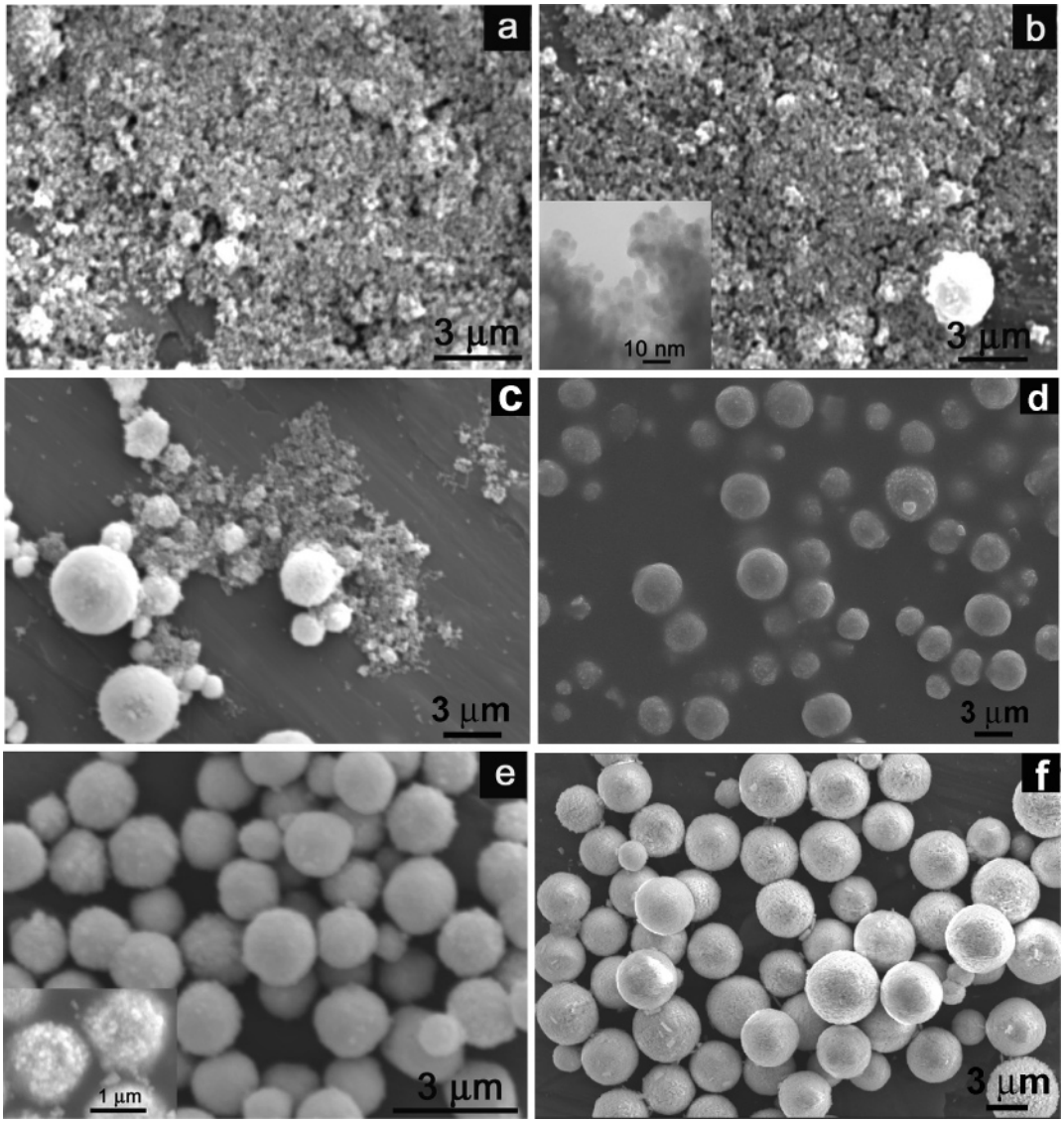

Figure 2. SEM images of $PbTiO_3$ products prepared by the hydrothermal method from Pb−Ti−citrate sol without surfactant at (a) 90 °C, (b) 100 °C, (c) 110 °C, (d) 130 °C, (e) 150 °C, and (f) 180 °C for 24 h. Insets in parts b and e correspond to the detailed view of the sample with the TEM and FESEM image, respectively.

an amorphous product after 24 h at 150 °C. By increasing the reaction time to 48 h, $PbTiO_3$ microspheres with uniform size of 1−2 μm were obtained. Increasing the CTAB concentration to 0.4 M, $PbCO_3$ was obtained after 24 h at 180 °C. However, using the dried gel instead of sol as the precursor, a mixture of tetragonal $PbTiO_3$ and cubic $Pb_2Ti_2O_6$ were formed. The morphology of the products was nanoparticles, and no microspheres or bur-like nanostructures were observed. The synthesis conditions and morphology of the produced bur-like nanostructures prepared by using the surfactant SDBS or PSS are summarized in Table 1.

The nanorods could be broken off the core microspheres by grinding by hand for about 3 min using a mortar or by ultrasound treatment in ethanol. This indicates that the bur-like $PbTiO_3$ nanostructure contains a core−shell structure with areas of structural weaknesses between the core and the shell. The separated nanorods could be further broken down into smaller particles by increasing the grinding time, showing that the as-prepared nanorods had low mechanical strength.

The microstructure of the bur-like $PbTiO_3$ nanostructures synthesized after 48 h at 180 °C using 0.2 M SDBS was further investigated by TEM. The low-magnification TEM image of the typical bur-like $PbTiO_3$ nanostructures (Figure 5a) confirmed that the diameter of the microsphere surrounded by nanorods is $\sim$ 2 μm. The nanorods, where a typical one is shown in Figure 5b, had a diameter of 30−100 nm and a length up to 1 μm. The corresponding selected area electron diffraction (SAED) pattern (inset in Figure 5b) demonstrated that the nanorods grow along the [001] direction. A high-resolution TEM (HRTEM) image of the outer tip of the nanorod (Figure 5c) shows lattice spacings of 0.41 nm in the length direction of the rod, which corresponds to the distance between two (001) $PbTiO_3$ crystal planes, confirming the [001] growth direction. The shape of the rods tapers from the bottom to the top. The nanorods are covered by a $\sim$4 nm amorphous organic layer, which is proposed to be a layer of the surfactant. The surfactant layer is important for the growth mechanism as discussed further below. EDS analysis of a nanorod confirmed that the rod

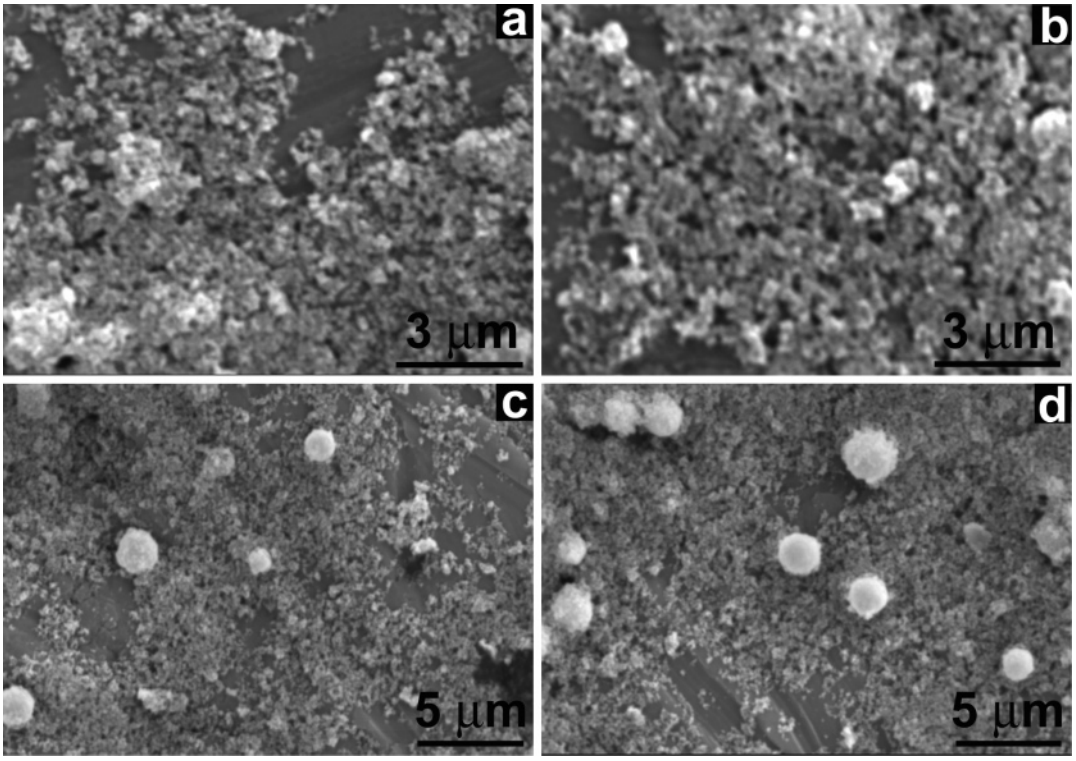

Figure 3. SEM images of $PbTiO_3$ products prepared by the hydrothermal method from Pb−Ti−citrate sol without surfactant at 100 °C for (a) 6 h, (b) 12 h, (c) 24 h, and (d) 48 h.

was composed of Pb, Ti, and O (Figure 5d).

Cross-section samples of the bur-like nanostructures were investigated to study the internal structure of the bur-like nanostructures. A typical TEM image is shown in Figure 6a and revealed that the core microspheres were porous and composed of $PbTiO_3$ nanocrystals (see SAED pattern inset) while the $PbTiO_3$ nanorods grew outward from the surface of the porous core. Figure 6b confirms that the microspheres are indeed porous clusters of nanoparticles and indicates that there might be two types of microspheres, one with a uniform distribution of nanoparticles (shown by the arrow) and the other with regions of different particle densities. Nanorods were not found at the microspheres that have a uniform distribution of the nanoparticles, while the microspheres containing regions with clustered nanoparticles formed bur-like nanostructures. In some of the bur-like nanostructures a uniform distribution of nanoparticles was found in the interior of the microsphere, while the outer part of the microsphere consisted of areas with varying particle density. The polycrystallites in the microspheres seem to have preferred orientations. A low magnification TEM image that shows the cross-section of many nanorods is given in Figure 6c. The cross-section of these nanorods is rectangular. Near the microspheres, the nanorods have irregular outer surfaces and pores inside (Figure 6d). However, toward the tip, the structure is regular and defect free as shown in Figure 6e. Defects observed in the nanorods close to the microsphere suggest that they originate from oriented self-assembly of cube-shaped or facetted nanocrystals.[14a,15] The HRTEM image in Figure 6f reveals that the nanorods are built up by nearly rectangular nanocrystals ($\sim 10 \times 10$ nm^2) as the building blocks. These assembled nanocrystals form mesocrystals.[15]

4. Discussion

4.1. Growth Mechanism of $PbTiO_3$ Microspheres. Upon hydrothermal synthesis of the $PbTiO_3$ microspheres, crystalline $PbTiO_3$ nanoparticles (about 5 nm) were formed for reaction times longer than 6 h and temperatures higher than 90 °C (Figure 1−3). At lower temperatures and for shorter reaction times, only amorphous particles were obtained (Figure 1). When the reaction temperature is increased (>90 °C) or the reaction time is prolonged, the primary nanoparticles grow and aggregate to $PbTiO_3$ microspheres, which become more uniform with increasing reaction temperature. From these observations, the most plausible mechanism for the growth of the monodisperse microspheres is that nanoparticles nucleate, grow, and aggregate. Growth of the nanoparticles may obey the classical model for growth;[16] however, aggregation into larger units follows other growth kinetics like the Smoluchowski's equation.[17] For the aggregates to form perfect spheres, there must be sufficient short-range repulsion due to surface charge in the highly basic environment between them to allow the particles to settle into the microspheres in addition to high concentration of primary particles. For nanoparticles that carry a

(15) Cölfen, H.; Antonietti, M. *Angew. Chem., Int. Ed.* **2005**, *44*, 5576−5591.

(16) (a) LaMer, V. K.; Dinegar, R. H. *J. Am. Chem. Soc.* **1950**, *72*, 4847−4854. (b) Brinker, C. J.; Scherer, G. W. *Sol-Gel Science: The Physics and Chemistry of Sol-Gel Processing*; Academic: London, 1990; pp 270−284.

(17) Brinker, C. J.; Scherer, G. W. *Sol-Gel Science: The Physics and Chemistry of Sol-Gel Processing*; Academic: London, 1990; pp 331−333.

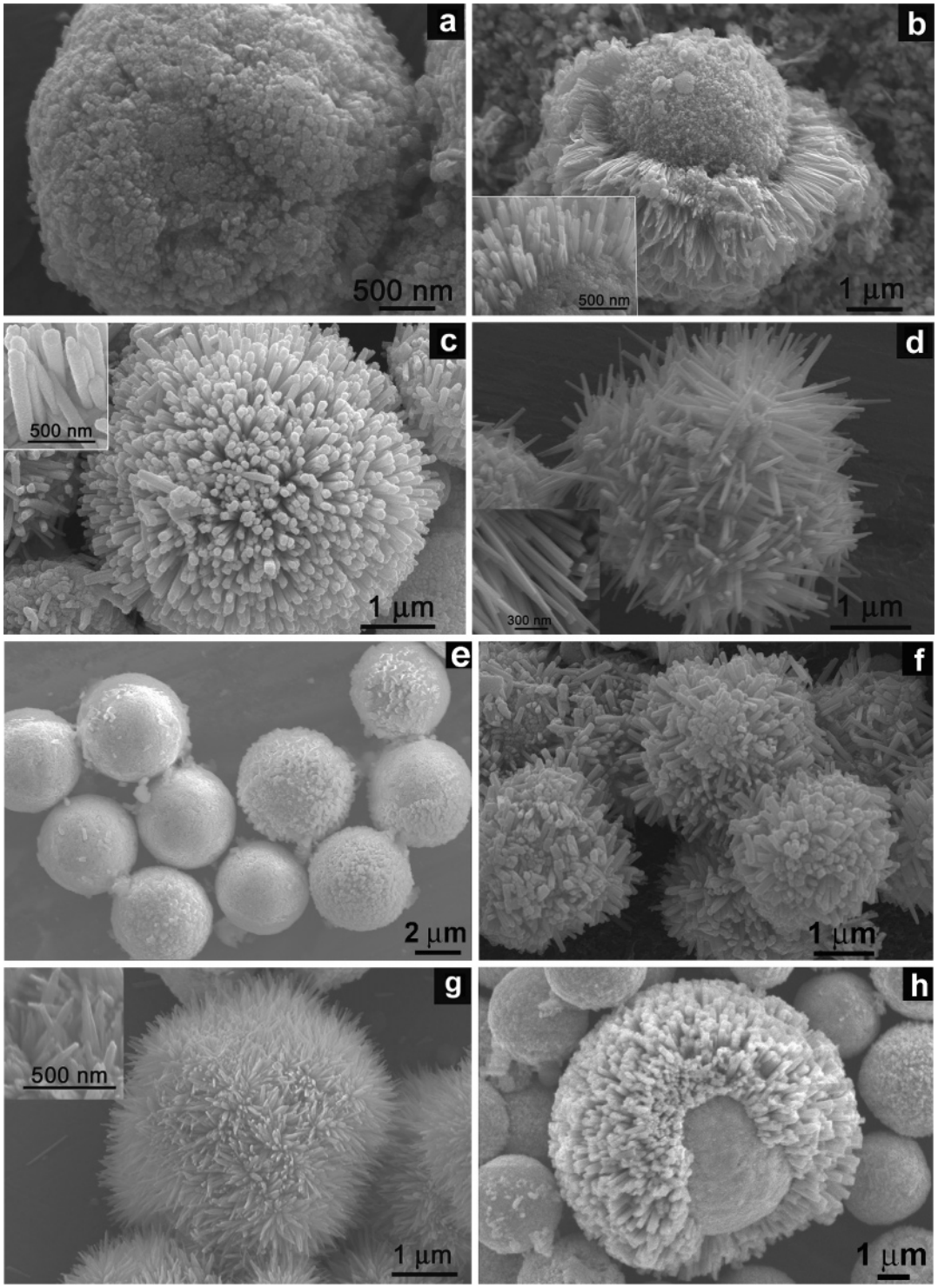

Figure 4. SEM images of $PbTiO_3$ nanostructures prepared by the hydrothermal method from Pb−Ti−citrate sol for 48 h. (a−d) With different SDBS concentrations at 180 °C: (a, b) 0.1 M, (c) 0.2 M, and (d) 0.3 M. (e) Without surfactant at 180 °C. (f, g) with 0.2 M SDBS concentration at different temperatures, (f) 150 °C and (g) 200 °C. (h) 0.2 M PSS concentration at 180 °C. Insets in images are selected parts imaged at higher magnification.

surface charge, small clusters of nanoparticles aggregate more quickly with large aggregates than they do with themselves. Consequently, during the reaction, the first nanoparticles aggregate to form microspheres. These microspheres then sweep through the solution, picking up freshly formed nanoparticles. Monodisperse microspheres of the final precipitate are achieved. Presence of EG in the Pb−Ti−citrate sol precursor was shown to be necessary for the aggregation leading to the formation of microspheres. EG is expected to bind the nanoparticles together through ester bond formation after the aggregation has taken place.

4.2. Growth Mechanism of Bur-like $PbTiO_3$ Nanostructures. The mechanism for the formation of the $PbTiO_3$ bur-like nanostructures is proposed to involve different growth processes during the hydrothermal synthesis as schematically illustrated in Figure 7: (i) initial nucleation and (ii) growth of $PbTiO_3$ nanoparticles, (iii) formation of

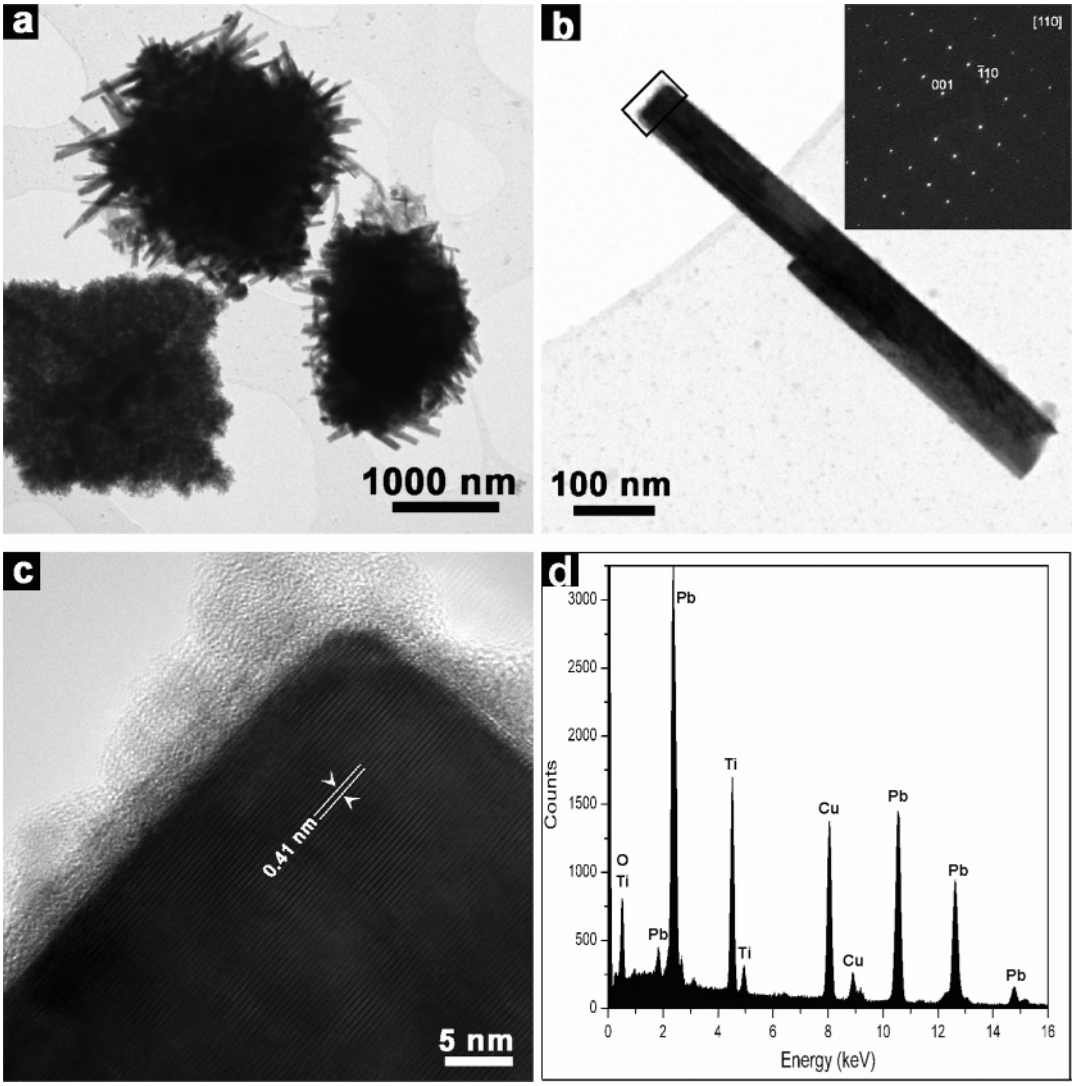

Figure 5. (a) TEM image of the bur-like nanostructures. (b) $PbTiO_3$ nanorod and SAED pattern (inset). (c) HRTEM image of the tip of the rod in part b. (d) EDS spectrum of this nanorod showing the Pb, Ti, and O peaks; the Cu signal originates from the TEM grid.

Table 1. Summary of Results from the Synthesis of Bur-like $PbTiO_3$ Nanostructures during Hydrothermal Synthesis for 48 h at pH ≥ 14 Using a Pb−Ti−Citrate Sol as Precursor with Surfactant.

synthesis conditions		results		
			size of nanorod	
temperature (°C)	surfactant type/concentration (M)	morphology	diameter (nm)	length (μm)
150	SDBS/0.2	bur-like nanostructures with nanorods of different lengths	several hundred	<1
180	SDBS/0.1	bur-like nanostructures and microspheres	30−100	<1.5
180	SDBS/0.2	bur-like nanostructures with uniform nanorods	30−100	~1
180	SDBS/0.3	bur-like nanostructure with prismatic tetragonal nanorods	~70	~2
200	SDBS/0.2	bur-like nanostructures with needle-like nanorods	~80	~1.5
180	PSS/0.2	bur-like nanostructure with prismatic tetragonal nanorods	~240	~1

the core of the bur-like $PbTiO_3$ nanostructures by aggregation of the primary $PbTiO_3$ nanoparticles into microspheres, (iv) ripening of the nanoparticles to nonspherical building blocks or continued nucleation of nanoparticles with facetted or cube shape, and (v) self-assembly of the $PbTiO_3$ building blocks onto the microsphere surface to mesocrystals which further (vi) ripen to nanorods. The microspheres, hence, act as substrates for the growth of the nanorods.

In step iii, $PbTiO_3$ nanoparticles aggregate into the microspheres, which act as substrates for nanorod growth and become the core of the bur-like nanostructures. The growth process of the core is similar to that of microspheres formed in the absence of the surfactant, which can be seen by comparing parts a and e of Figure 4. The partly destroyed bur-like nanostructure shown in Figure 4b confirms that the nucleation of the nanorods is taking place on the surface of the microsphere with radial growth of the nanorods (inset of Figure 4b).

Further, mesocrystals of $PbTiO_3$ were formed by self-assembly of the cube-shaped or facetted nanocrystals onto the microsphere substrate, step v. The evolution of size and shape of the nanocrystals dispersed in the reaction mixture

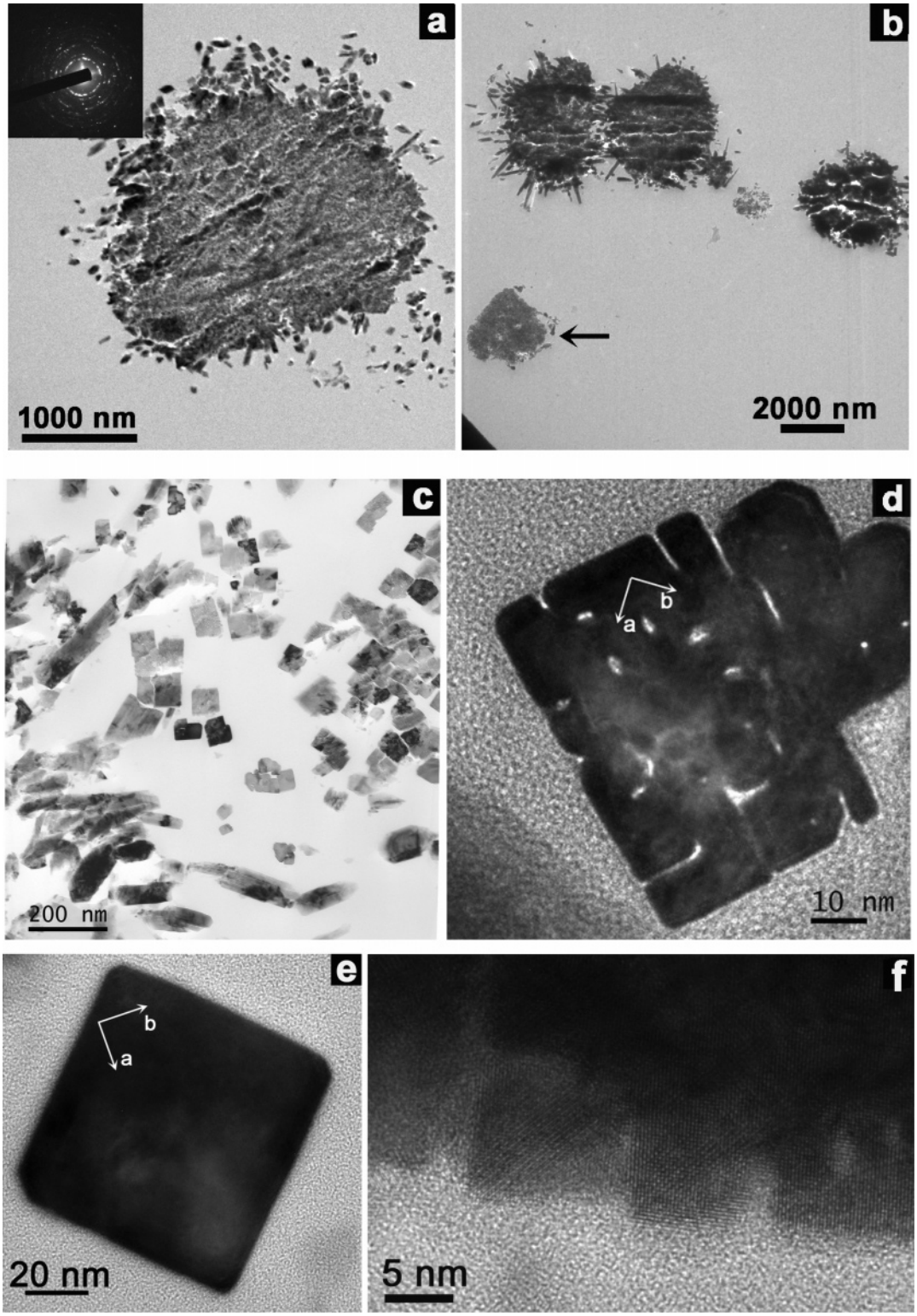

Figure 6. TEM images of a cross-section: (a) a bur-like nanostructure with SAED (inset), (b) microspheres with or without nanorods, (c) a number of nanorods, (d) a rod cut close to the microsphere, and (e) a rod near the tip. (f) HRTEM image of the edge of a rod in cross section, showing the nanocrystals.

is further discussed below. Figure 6f indicates parallel crystallographic orientations between primary building block neighbors. As tetragonal $PbTiO_3$ is ferroelectric and has a dipole moment along the *c*-axis, the anionic surfactant can be selectively adsorbed onto the charged (001) face of a $PbTiO_3$ nanocrystal. This dipole moment leads to the observed stacking of nanocrystals into mesocrystals. The driving force for the self-assembly is proposed to be the entropy gain (increase in free volume) by the release of adsorbed surfactants and decrease in surface energy. Defects observed in the nanorods close to the microsphere core confirm that the nanorods originate from oriented self-assembly of cube-shaped or facetted nanocrystals (Figure 6d).[3a,15,18] Continuous growth of the mesocrystal followed by ripening gives rise to the final crystalline nanorods

(18) (a) Song, Q.; Zhang, Z. J. *J. Am. Chem. Soc.* **2004**, *126*, 6164−6168. (b) Jun, Y. W.; Choi, J. S.; Cheon, J. W. *Angew. Chem., Int. Ed.* **2006**, *45*, 3414−3439.

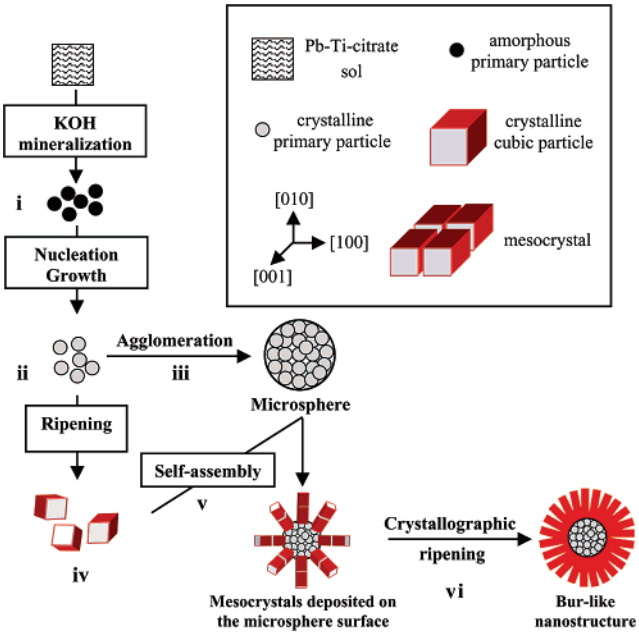

Figure 7. Schematic drawing illustrating the mechanism for the bur-like nanostructure growth.

growing out from the microspheres. The above findings are in agreement with the observation made by other researchers in growing metal oxalate hierarchical structures, where a multiple-stage process has also been proposed.[19]

It is interesting to note that the building blocks of the microspheres were irregular or spherical nanoparticles, while the building blocks of the nanorods are cube-shaped or facetted nanocrystals. We therefore conclude that there occurred an evolution of the shape and size of nanoparticles in the solution over time. The morphology and size of these nanoparticles might become more regular as a result of ripening, for example by change in saturation level of the solution giving cube-shaped or facetted nanoparticles over time. Alternatively the nucleation of new particles/crystals occurs continuously through of the synthesis and the nucleated particles become more and more cube-shaped or facetted with time as a result of the decreasing super-saturation. A change in viscosity in the solution might also influence on the size and morphology of the nucleated nanocrystals.[15,18] According to the polar crystal growth theory of Hartman and Bennema,[20] {100} planes in $PbTiO_3$ are considered to be the slowest growing planes; thus, the particles tend to grow into an anisotropic shape, resulting in the cube-like particles.[3a]

Selective adsorption of the surfactant onto the nanocrystal surface is probably dependent on nanocrystals with well-defined crystallographic planes, for example, for cube-shaped or facetted nanocrystals. At least for the surfactant to aid in the self-assembly of the nanocrystals into mesocrystals, a well-defined shape of the nanocrystals is necessary. Only $PbTiO_3$ microspheres were formed under hydrothermal conditions without surfactant at 180 °C for 48 h (Figure 4e) showing that the presence of surfactants SDBS or PSS was necessary to form the bur-like nanostructures. These two surfactants have the same phenyl-sulfonic groups. The use of anionic and cationic surfactants CTAB, SDS, NPP, or CSS, which do not have the phenyl-sulfonic groups, did not result in formation of nanorods. Only a selective choice of surfactant is aiding the nanorod and bur-like nanostructure formation.

The nanorods have perfect prismatic tetragonal shape using high SDBS concentration (see Figure 4d). This might be attributed to the fact that the viscosity of the solution becomes larger with increasing the surfactant concentration. This increased viscosity might slow down the nanoparticle movement, giving more time for the particles to diffuse on the surface and adjust before being incorporated into the lattice. Nanorods with the needle-like shape were found (see Figure 4g) at high temperature, which might be due to different growth rates of the various faces. All nanorods have the characteristic shape tapering from the bottom to the top, which should be attributed to the gradual exhaustion of solute and the decreasing rate of $PbTiO_3$ nanoparticle nucleation. It is evident that the nanorods can be modulated by the surfactant concentration and reaction temperature.

4. Conclusion

We have demonstrated the formation of novel hierarchical bur-like $PbTiO_3$ nanostructures formed by self-assembly of nanocrystals by using the surfactants SDBS or PSS under hydrothermal conditions. In the absence of these surfactants, 1−4 μm monodisperse microspheres, consisting of ∼20 nm $PbTiO_3$ nanoparticles, were formed. It was shown that EG was necessary for the formation of the microspheres. The microspheres worked as substrates for growth of single-crystalline $PbTiO_3$ nanorods resuting in novel hierarchical bur-like nanostructures. The $PbTiO_3$ nanorods were shown to grow out from microspheres along the [001] direction. A two-step process is proposed for the growth mechansim: The first step is agglomeration of $PbTiO_3$ nanoparticles into microspheres. The second step is self-assembly of nanosized cube-shaped or facetted building blocks into $PbTiO_3$ mesocrystals which continuously grow into nanorods. A prerequisite for the self-assembly of the nanoparticles into nanorods was the presence of the surfactant SDBS or PSS containing phenyl-sulfonic groups. This facile method offers the possibility for the production of complex, dipolar ternary oxide 1D nanostructures. Such structures have the potential to be building components for functional nanostructures and are also potentially interesting for 1D property studies at the nanometer scale.

Acknowledgment. The authors wish to thank Bjørn S. Tanem from SINTEF Materials and Chemistry for making the microtomed TEM sample. The work was financed by the Research Council of Norway (NANOMAT-program, Grant 158518/431).

CM063047D

(19) (a) Pujol, O; Bowen, P; Stadelmann, P. A.; Hofmann, H. *J. Phys. Chem. B* **2004**, *108*, 13128−13136. (b) Soare, L. C.; Bowen, P.; Lemaitre, J.; Hofmann, H. *J. Phys. Chem. B* **2006**, *110*, 17763−17771.
(20) Hartman, P.; Bennema, P. *J. Cryst. Growth* **1980**, *49*, 145−156.